International Journal of Modern Physics A
Vol. 24, No. 5 (2009) 908–922

World Scientific
www.worldscientific.com

HIGH-ORDER DESCRIPTION OF THE DYNAMICS IN FFAGs AND RELATED ACCELERATORS

KYOKO MAKINO,* MARTIN BERZ,† PAVEL SNOPOK‡ and CAROL JOHNSTONE§

Department of Physics and Astronomy, Michigan State University,
Fermi National Accelerator Laboratory, USA
Department of Physics and Astronomy, University of California Riverside, USA
**makino@msu.edu*
†*berz@msu.edu*
‡*snopok@gmail.com*
§*cjj@fnal.gov*

In this paper, we describe newly developed tools for the study and analysis of the dynamics in FFAG accelerators based on transfer map methods unique to the code COSY INFINITY. With these new tools, closed orbits, transverse amplitude dependencies and dynamic aperture are determined inclusive of full nonlinear fields and kinematics to arbitrary order. The dynamics are studied at discrete energies, via a high-order energy-dependent transfer map.

The order-dependent convergence in the calculated maps allows precise determination of dynamic aperture and detailed particle dynamics. Using normal form methods, and minimal impact symplectic tracking, amplitude- and energy-dependent tune shifts and resonance strengths are extracted. Optimization by constrained global optimization methods further refine and promote robust machine attributes.

Various methods of describing the fields will be presented, including representation of fields in radius-dependent Fourier modes, which include complex magnet edge contours and superimposed fringe fields, as well as the capability to interject calculated or measured field data from a magnet design code or actual components, respectively.

Keywords: FFAG; differential algebra; COSY INFINITY; dynamic aperture; symplectic tracking.

PACS numbers: 29.20.D-, 29.20.dg, 29.27.Bd, 87.56.bd, 41.85.Lc, 41.75.Lx, 41.75.-i

1. Introduction

The broad class of FFAG-type accelerators is experiencing an international revival in the quest for high beam power, duty cycle, reliability and, in the case of the spiral-sector FFAG, the potential for compactness at reasonable cost.[1,2,3,4,5] The FFAGs proposed have the high average current and duty cycle characteristic of the cyclotron combined with the smaller aperture, losses, and energy variability of the synchrotron. Although new accelerator prototypes are often simulated with conventional tracking codes, these codes do not provide much flexibility in the field

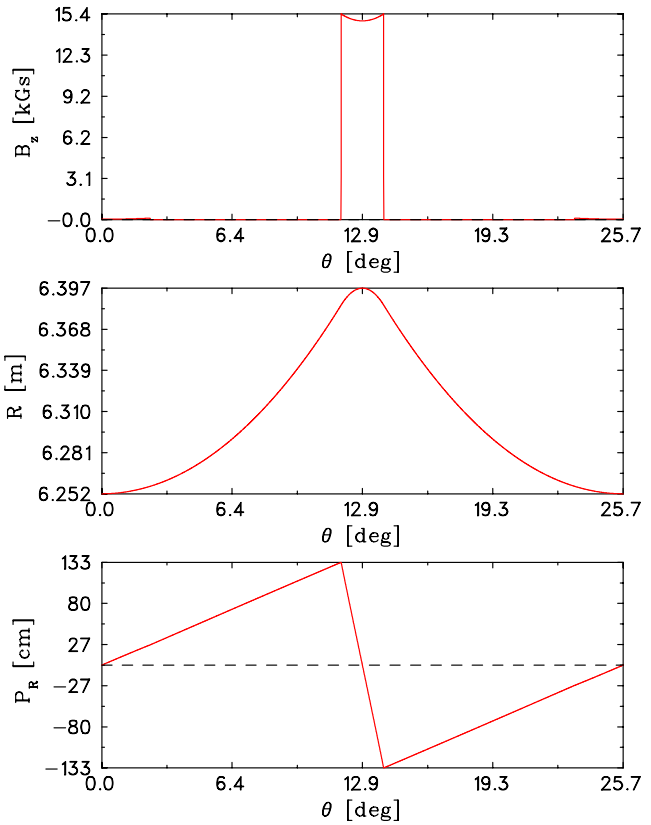

Fig. 1. B_z (vertical) field at injection for nonscaling FFAG lattice showing sharp cutoff of field at end of CF magnet, along with the radius of the injected orbit along the periodic cell and the angle as measured with respect to a normal projection relative to a radial line.

description and are limited to low order in the dynamics. This limitation can be inadequate to fully demonstrate performance including dynamic aperture where strong nonlinearities due to edge fields and other high-order effects appear. This is particularly true for the FFAGs. In the muon FFAGs, for example, the large beam emittances require the inclusion of kinematical (or angle) effects in the Hamiltonian, which implies that codes which fully describe the kinematics are necessary.[6,7]

The current number of supported design and optimization codes that can adequately describe the complex field and magnet contours for both the scaling and nonscaling FFAG variants is limited. Outside of COSY, present public codes include only the cyclotron code CYCLOPS,[8] and the field-map code ZGOUBI.[9,10] The former, which utilizes fields and their geometry expanded in polar coordinates, has limited accuracy in this application primarily due to lack of out-of-plane expansion order, and in handling of edge-field effects; this is particularly true for the case of rapid azimuthal field fall off at magnet edges (as in the FFAG field profile of Fig. 1), an effect not present in cyclotrons. The results and derived performance

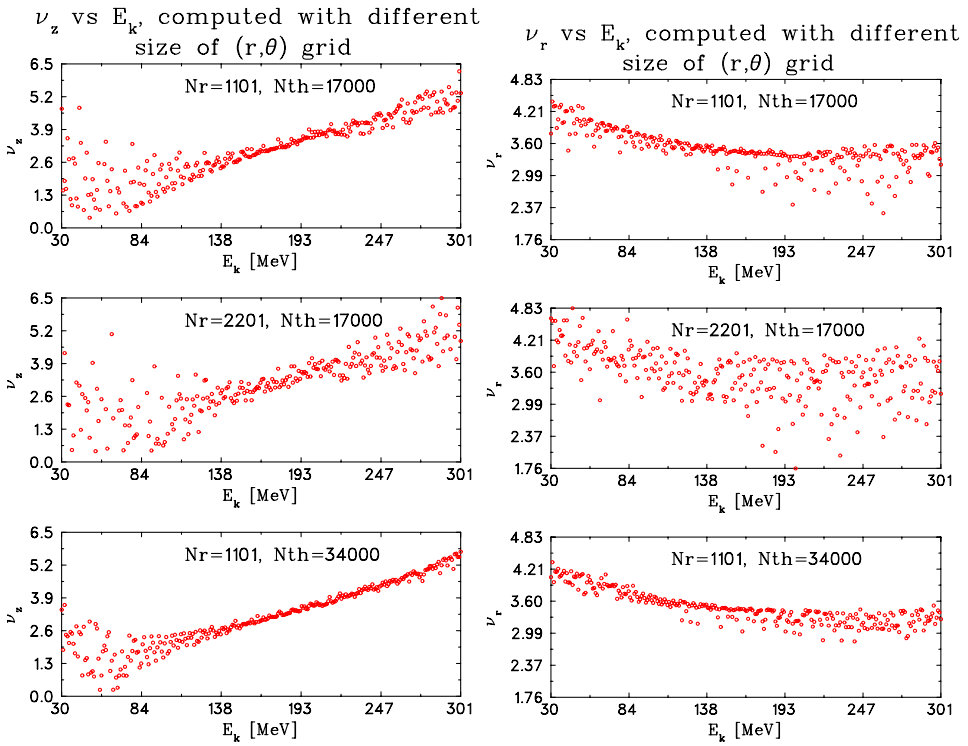

Fig. 2. Radial and azimuthal tunes for a 14-cell, 30–400 MeV nonscaling proton FFAG showing dependence on number of radial (N_r) and azimuthal (N_θ) mesh points used in field calculation.

can be strongly dependent on the integration step size across such an edge with Fig. 2 showing results for different mesh sizes. Since Cyclops remains a cyclotron code, it does not directly incorporate field data, either calculated or measured, primarily derives only closed orbits and tunes for an FFAG, and has no standard models to handle fringe fields. (Particle tracking and dynamics require another associated code.) The latter code, ZGOUBI, is presently being used successfully in FFAG development, but requires dedicated effort and expertise to implement an FFAG design, particularly when expressed in terms of the conventional magnetic component definitions. At present, some modern analysis tools for symplectic tracking, global optimization, tuneshifts and chromaticities, and resonance analysis are not as yet available.

In the following an analysis of a 14-cell, linear-field nonscaling 400-MeV FFAG for protons is compared between MAD, ZGOUBI, and CYCLOPS. (In MAD, the simulations were performed at discrete energies based on a derived closed orbit.) The results from MAD reflect a simple hard-edge. Field modeling in Cyclops reflected the hard edge representation, but experienced difficulty in calculating tunes with strong sensitivity to the fineness of mesh size discretization near the edge (Fig. 2). A considerable degree of effort[11] was expended in ZGOUBI to effect both the edge

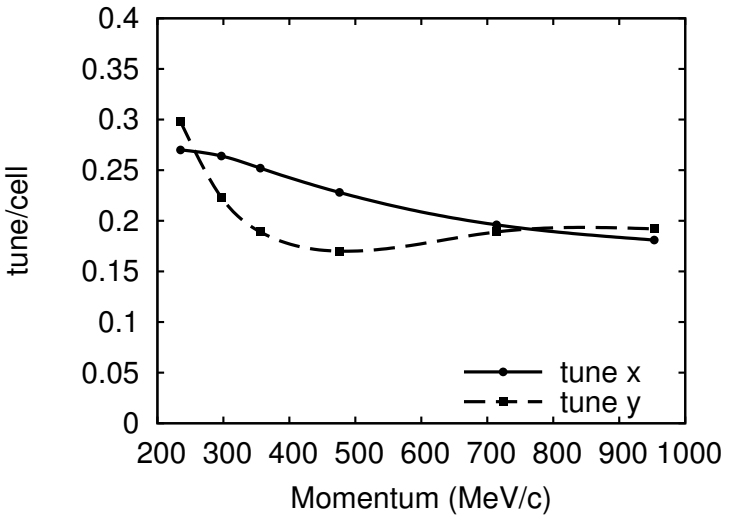

Fig. 3. Dependence of cell tune on momentum in an example of a nonscaling, linear-field FFAG which is tune-stabilized about 90°. Solution obtained from the approximated equations.

contour and a hard edge in order to reproduce the MAD model and results. (The parameters of the Enge function, the convention in ZGOUBI for the fringe-field model, were adjusted by hand to emulate a hard-edge fall-off.) The final tune dependence in the figure reflects repetitive tuning of the edge angle, again by hand, to most closely reproduce the desired results of the simpler MAD simulation. Figs. 3–5 show the MAD and final ZGOUBI results for this specific lattice. Tune dependence of the 14-cell ring modeled in Cyclops using the field and edge profile of Fig. 1 at injection coupled to the design linear-field gradient and linear edge specified in the design model is shown in Fig. 2. Note the sensitivity and large distribution in the tune calculation, especially at low-field points.

Modern extensions of the transfer map-based philosophy[12,13] as implemented in the arbitrary order code COSY INFINITY[14,15] address both limitations: high-order and accurate dynamics. Yet, the standard field configurations which, in turn, are based on the standard complement of accelerator components are not able to realize a general description for the FFAG concept—such as combined function magnets with complex edge and/or nonlinear field profiles.

Further, in promoting advanced accelerator design, the ability to perform extended parameter optimization has become increasingly important, if not critical. Although effective optimization requires initial conditions that rely on educated, experienced choices by the designer, subsequent manual adjustment and local optimization are rarely fully optimal and often fail for advanced accelerators such as the FFAGs. Large-scale global optimization, which not only probes local neighborhoods, additionally searches over extended domains of parameter space for suitable solutions. Recent significant advances in global optimization,[16,17,18,19,20] illustrated

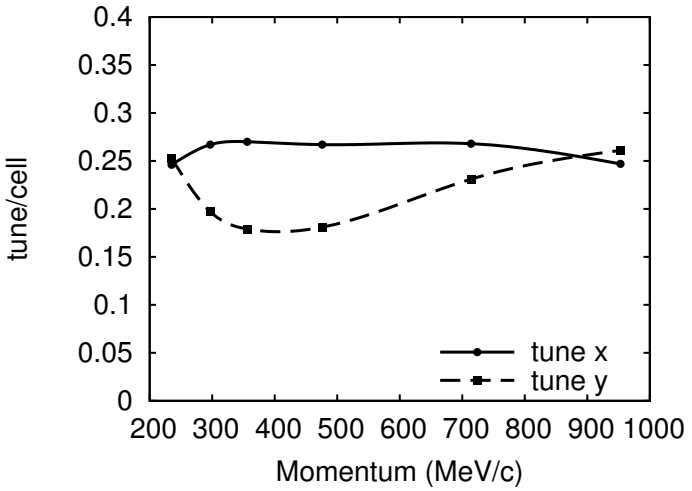

Fig. 4. Dependence of cell tune on momentum in an example of a nonscaling, linear-field FFAG which is tune-stabilized about 90°. Tune as modeled in MAD.

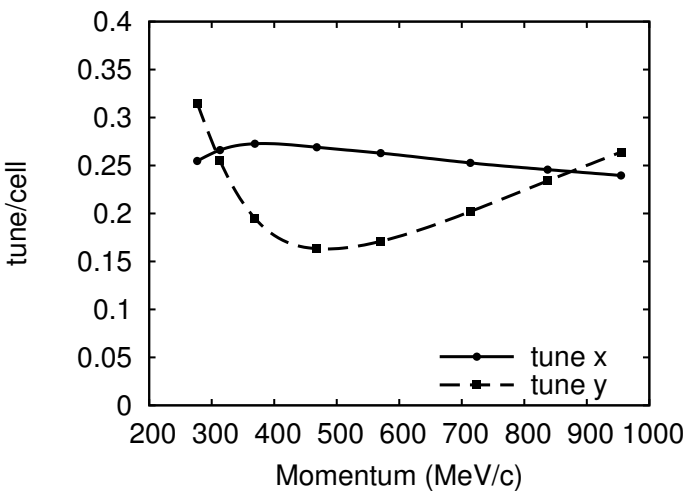

Fig. 5. Tune dependence of the nonscaling, linear-field FFAG in the code ZGOUBI as initially modeled in MAD (previous figure) for a single cell. Significant adjustment of edges and Enge-function parameters was required to achieve approximate agreement with the intended design described by the MAD simulations and analytical approximations.

by the various different directions of cutting edge research including genetic optimization, divide and conquer approaches, and verified methods, have led to a state of the art in optimization such that they significantly simplify and promote the design process. Further, they can prove critical in achieving a robust, state-of-the art design both in dynamical performance and technical criteria for critical accelerator technologies such as the FFAGs.

In the following, methods are described that allow the description and analysis of FFAGs and related types of accelerators. The approaches developed have the capability to model the wide array of FFAG design parameters and complicated fields in the presence of very large emittance beams. Description of arbitrary field profiles will be presented, including a representation in radius-dependent Fourier modes, which include terms describing the effects of magnet edges along with superimposed fringe fields from the different modes. Alternatively, data from magnet design codes and field measurements can be used in place of these representations.

2. Field Models

In the following various methods are discussed to describe the transverse focusing properties of FFAGs and how these methods are applied over the full acceleration range. The methods differ in level of sophistication and accuracy, as demanded by the level of complexity of the design fields and physical configuration of the individual components.

2.1. *General Combined-Function Magnets in COSY*

In a number of specific cases it is possible to describe an FFAG lattice in terms of standard COSY beamline elements. For these machines an extended set of combined function magnets have been implemented both with tilted and curved entrance edges and a choice of conventional fringe field models. Alternatively, actual data, either measured or from a magnet design code, can be entered for a calculation using exact fringe fields. The description of these elements allow a rather sophisticated level of design as long as the fields of individual elements do not strongly overlap (implying interaction between components and unnatural fringe fields) and as long as the field profiles are not unusual or extreme functions of radius or azimuthal angle. For details we refer to [14].

The disadvantage of this approach is that it is based on a description relative to a reference orbit and therefore relies on the deflection properties about this orbit. Studying multiple reference energies, as must be done for an FFAG, makes for a rapidly expanding problem dimensionally and one that quickly becomes difficult to analyze. To counter this expansion, in the next sections, we provide field descriptions in terms of a laboratory-based coordinate system that applies to all possible reference orbits and reduces the descriptive magnitude of the problem.

2.2. *Generalized FFAG Magnets*

An enhancement of the above approach that provides greater flexibility and control, entails the superimposition of combined-function (CF) magnets. A "universal" FFAG magnet can be effectively described in terms of superimposed CF magnets with arbitrary, high-order (individual multipole) fields. Each overlay retains the required complex edge curves and associated high-order dynamics. This approach is

new in that the effective centers of the constituent multipoles do not have to coincide physically in the CF magnet. This approach produces a truly arbitrary field profile which is difficult or impossible to reproduce in other codes.

Further, since FFAGs have completely periodic lattices, it is sufficient to define a "half cell" for a repetitive simulation; that is, the structure is defined from one reflective symmetry point to another. Geometric closure of an orbit requires that all orbits, even off-reference ones, must be parallel at such points, or "reflection" does not hold; i.e. all derivatives must be zero for stable orbits. Hence it is sufficient to construct only a half cell map from which the full cell map is automatically generated. In the full cell, the model extends from one symmetry point at the center of a CF magnet, past the next to the same symmetry point in the identical CF magnet in the sequence. For the half cell, the model extends only to the next symmetry point—from the center of the horizontally focusing CF magnet to the center of the horizontally-defocusing CF magnet, for example. The remaining half of the full cell is generated by reflection to find closed orbit and optical properties at any energy and for tracking of particle distributions.

In this manner, the full FFAG can be constructed from $2n$ sector-shaped half cells, each of which has a sector angle of π/n. The $2n$ half cells are arranged in n identical pairs consisting of one half cell and its mirror image to form the full periodic unit, or full cell. As a consequence of this symmetry, all closed orbits therefore cross the half cell boundaries perpendicularly and parallel to one another. The lines normal to the orbits at these symmetry points actually form a radial line to the geometric center of the FFAG.

Within each full cell, there are either two or three magnets, depending on the FFAG base unit cell, a FODO, doublet, or triplet structure, and each magnet has a radial field profile $B_{y,i}$ given by

$$B_{y,i} = B_{0,i} \cdot P_{B,i}(r)$$

where $B_{0,i}$ is a reference field value and $P_{B,i}$ is a dimensionless polynomial in the polar radius r.

The magnets are bounded by curves describing their effective field boundaries. Specifically, the first magnet is bounded by the exit curve P_{12}; note that the repeated mirror symmetric arrangement entails that its entrance curve is also specified by P_{12}. The second magnet is bounded by the entrance curve P_{21}. In the two-bend case, P_{21} also defines the exit curve due to the imposed mirror symmetry. In the three-bend case, the exit curve of the second bend is specified by P_{22}, and the entrance curve of the third bend is specified by P_{31}. The details of the arrangements are shown in Fig. 6.

All curves in the (x, z) midplane are represented in terms of a parameter t in the form

$$(x, z)_{ij}(t) = \vec{P}_{ij}(t) \text{ where } t \in [0, 1]$$

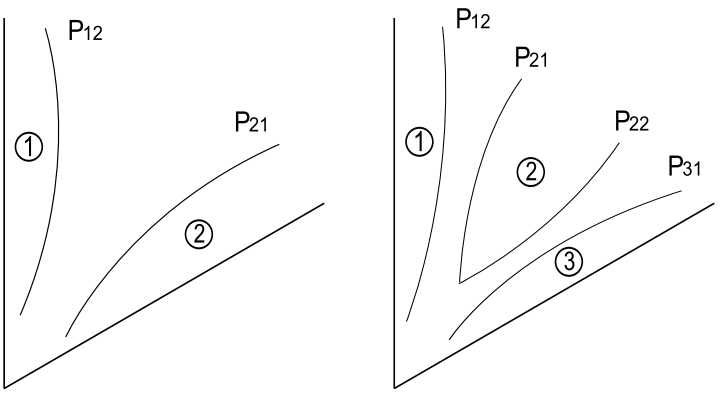

Fig. 6. The curves describing the effective field boundaries of the FFAG magnets in a cell of angle π/n in the two-bend (left) and three-bend (right) case.

where the origin of the coordinate system is at the center of the accelerator. In the vicinity of an edge curve, the fringe field belonging to the magnet bounded by that curve is given by an Enge Function

$$B_y(x,z) = \bar{B} \cdot \frac{1}{1+\exp(P_i(d/D_i(r)))}$$

where $\bar{B}$ is the main field acting at the point closest to (x,z) on the effective field boundary and P_i is a polynomial. Note that $\bar{B}$ is the sum of the contributions from the individual multipoles. The quantity d is the distance of the point (x,z) to the effective field boundary, and D_i is the aperture of magnet i, which is allowed to vary with radius in polynomial form.

Enge functions provide significant flexibility for the description of most types of realistic field fall-offs by appropriately choosing the coefficients of the polynomial in the exponential function. Thus, fringe field profiles based on other explicit functions are usually not necessary, at least in early stages of design.

Fringe fields of neighboring curves are allowed to overlap. Overall, the fringe field description is very similar to the approach that has been followed very successfully in the study of high-resolution particle spectrographs.

The advantage of this particular field model is that it allows a relatively simple adjustment of the main parameters commonly studied in the design of FFAG magnets while providing a fully Maxwellian and realistic field description. Specifically, the radial field variation appearing in $P_{B,i}(r)$ affects both the horizontal and vertical focusing for quadrupole and higher fields and only horizontal focusing for dipole, and the edge curves $\vec{P}_{ij}(t)$ affect both horizontal and vertical focusing. The Enge fall off is well known to represent realistic field profiles which can be adjusted to accurately describe most magnets and can even approximate a rapid, hard edge fall-off which is useful for comparison with codes without fringing fields.

2.3. *Radius-Dependent Fourier Decomposition*

From the early days of the study of FFAGs (see for example [21, 22]), midplane fields are often described in terms of azimuthal Fourier modes. This description allows the capture of most of the effects relevant to the focusing while abstracting from the specific shapes of the magnets that provide the desired fields. We provide this option by allowing a field description of the form

$$B_y(r,\phi) = a_0(r) + \sum_{j=1}^{n} a_j(r)\cos\left(j(\phi-\phi_0(r))\right) + \sum_{j=1}^{n} b_j(r)\sin\left(j(\phi-\phi_0(r))\right).$$

The Fourier coefficients $a_j(r)$ and $b_j(r)$ as well as the phase angle $\phi_0(r)$ are described in terms of polynomials in r. Higher values of n obviously allow for more faithful modeling, while all of the common focusing effects can be observed already for lower values of n.

In some instances it is desirable to capture more radial detail than can be revealed by the polynomials $a_j(r)$ and $b_j(r)$. Specifically, let us assume we are given a table of a_{ij} on a grid of equidistant radii $r_i = i \cdot \Delta r$, let P_j be the polynomial of best fit to all data points, and let $\bar{a}_{ij} = a_{ij}/P_j(i\Delta r)$. We then perform a Gaussian wavelet interpolation[23] of the form

$$a_j(r) = P_j(r) \cdot \sum_i \bar{a}_{ij} G_\sigma(r - i\Delta r)$$

where $G_\sigma(x) = \exp\left(-x^2/\sigma^2\right)/\sigma\sqrt{\pi}$ with $\sigma \approx 1.5\Delta r$.

2.4. *Gaussian Wavelet Representation of Polar Midplane Data*

Beyond the tools useful to quickly provide field models for the initial design phase, in addition it is possible to describe the fields in terms of three-dimensional field models of various levels of sophistication as soon as such field data are known. As a first step, let us assume we are given a field representation in terms of midplane data $B_y^{(i,j)}$ in polar coordinates r and ϕ on a regular polar grid with spacing Δr and $\Delta\phi$. The midplane field is then described in terms of these as a wavelet representation of the form

$$B_y(r,\phi) = \sum_{i,j} G_{\sigma r}(r - r_i) \cdot G_{\sigma\phi}(\phi - \phi_j) \cdot B_y^{(i,j)}$$

where the Gaussian wavelet G_σ has the form $G_\sigma(x) = \exp\left(-x^2/\sigma^2\right)/\sigma\sqrt{\pi}$, and σ is chosen as approximately $1.5\Delta r$ and $1.5\Delta\phi$, respectively. From the midplane representation, the field is then reconstructed by conventional out-of-plane expansion.

Note that this representation has some inherent limitations since the out-of-plane is sensitive to errors in the field data in the midplane. It should hence be used with caution only after the effect of such errors on the quality of the resulting expansion in the domain of interest is established. One way to remedy this situation is to utilize the midplane data to first obtain a Fourier representation as described in section 2.3. Another method is described in the next section.

2.5. *Field Representations from Three-Dimensional Data*

From a mathematical point of view, the knowledge of magnetic fields in the midplane is sufficient to determine the fields at any point in space based on a power series expansion. Specifically, Maxwell's equations impose well-known conditions on the Taylor coefficients that under the assumption of midplane symmetry allow the determination of out-of-plane coefficients from those in-plane. Using DA-based methods as described in for example [12], the process can even be fully automated to any order. However, any attempt of representing three-dimensional field data in terms of fields given only in the midplane is sensitive to measurement errors, since these can greatly affect any attempt of recovering high-order midplane derivatives.

It is thus desirable to utilize field descriptions that do not rely on the midplane data. Indeed, a much more favorable approach is the utilization of surface field data. As discussed in [24, 25, 26, 27], this approach has a tendency to smooth out any measurement errors and leads to more faithful three-dimensional representations.

Other field arrangements are potentially desirable in certain cases. For example, one may want to describe fields of air coil-dominated magnets directly based on a data file describing the geometry of pieces of the respective coils and their currents.[27,28,29] Furthermore, if it is deemed desirable, one can perform injection-to-extraction simulations by providing acceleration elements of varying degrees of sophistication, beginning from pillbox-type elements to more sophisticated analysis based on field harmonics.

3. Analysis Tools

Based on the field descriptions provided in the last section, there are various tools of the COSY environment that can be utilized for subsequent analysis.

- **Closed Orbits.** First, a set of closed orbits is being determined for a suitable collection of reference particle energies by optimization.
- **Arbitrary Order Maps.** For each of the closed orbits, a high-order energy-dependent transfer map around it is calculated. This includes all dynamics of the system to arbitrary order, including out-of-plane expansions of fields and any nonlinear terms in the Hamiltonian.[12,30]
- **Linear Properties of Maps.** For this local map, common linear beam functions including invariant ellipses and tunes near the closed orbit are determined.
- **Tracking.** The high-order transfer maps can be used to perform tracking to estimate the dynamic aperture, presence of resonances, etc. There are various methods to perform tracking in COSY that preserve the symplectic symmetry inherent in Hamiltonian systems, including methods that do so with minimal modifications based on the EXPO approach.[31,32,33]
- **Acceleration.** It is possible to describe the fields in terms of cavities of various sophistication, ranging from kicks over pillbox-type cavities to Fourier modes in space and time. Independent of the type of acceleration device used, in order

to study acceleration effects through such systems, the entire dynamic range in energy is sampled in steps of energy. For each such step, the map will be represented through a high-order map including energy dependence, and acceleration tracking is possible by suitably switching between maps.

- **Amplitude Dependent Tunes and Resonances.** In addition to the mere empirical study, there are various tools for analysis of nonlinear effects, including the normal form-based computation of high-order amplitude dependent tune shifts and resonances.[12]
- **Global Parameter Optimization.** COSY allows the automatic adjustment and optimization of arbitrary system parameters; and different from other tools, the search uses methods of global optimization with constraints over a prespecified search region, and not merely local optimization from a starting parameter setting.

4. Performance Examples

To provide an illustrative example of the behavior to be expected, we study a sample FFAG having sixfold symmetry, with focusing stemming from an azimuthal field variation expressed as a single Fourier mode as well as edge focusing. The system is studied to various orders of out-of-plane expansion, and conclusions about dynamic aperture are drawn. We show the results for orders three and five, which are typical for the situation of conventional out-of-plane expansion in codes like Cyclops. Because the DA method used in COSY[12] is not based on divided differences, the necessary in-plane derivatives can actually be calculated to any order desired with an accuracy that is always close to machine precision.[12]

The results of tracking without symplectification and with EXPO symplectification are shown in Figs. 7–12. Apparently symplectification greatly affects the dynamic aperture to be inferred in the system. Tracking is performed using the EXPO symplectification scheme which is known to minimize the alterations to the non-symplectic tracking results compared to other symplectification methods.

Figs. 7–12 show phase portraits in the $(x - a)$ plane (left) and the $(y - b)$ plane (right), where $a = p_x/p_0$, $b = p_y/p_0$ are normalized horizontal and vertical momenta correspondingly.

However, Figs. 11 and 12, which are both based on order eleven out-of-plane expansion, show significant additional effects and different dynamic aperture compared to the lower order cases as seen in Figs. 7 to 10, suggesting that the low order methods for out-of-plane expansion and dynamics are not sufficient to capture the details of the dynamics. It would in fact lead to an incorrect prediction of dynamic aperture, underestimating it in the horizontal direction and overestimating it in the vertical. Further increases in order beyond eleven do not significantly affect the details of the symplectic motion shown, but continue to influence the non-symplectic motion. A rough estimate reveals that in this particular case, the dynamics as seen in non-symplectic tracking seems to begin to stabilize around order 11, which is still rather easily obtained within the power of a modern workstation.

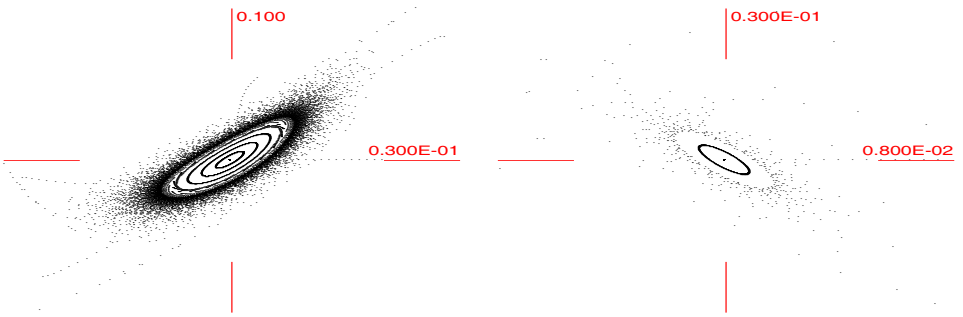

Fig. 7. Horizontal and vertical tracking in a model FFAG with third-order out of plane expansion, without symplectification. Left: $(x - a)$ plane, right: $(y - b)$ plane, where $a = p_x/p_0$, $b = p_y/p_0$ are normalized horizontal and vertical momenta correspondingly.

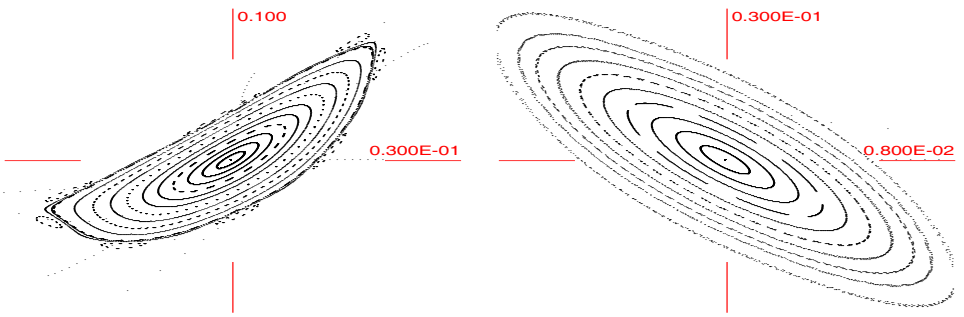

Fig. 8. Horizontal and vertical tracking in a model FFAG with third-order out of plane expansion, with EXPO symplectification. Left: $(x-a)$ plane, right: $(y-b)$ plane, where $a = p_x/p_0$, $b = p_y/p_0$ are normalized horizontal and vertical momenta correspondingly.

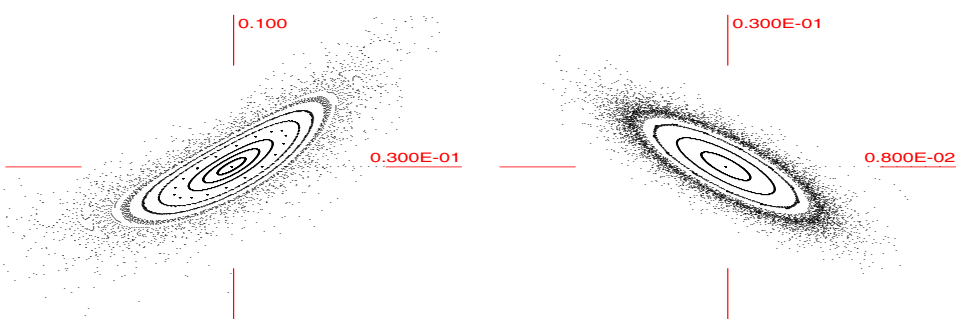

Fig. 9. Horizontal and vertical tracking in a model FFAG with fifth-order out of plane expansion, without EXPO symplectification. Left: $(x - a)$ plane, right: $(y - b)$ plane, where $a = p_x/p_0$, $b = p_y/p_0$ are normalized horizontal and vertical momenta correspondingly.

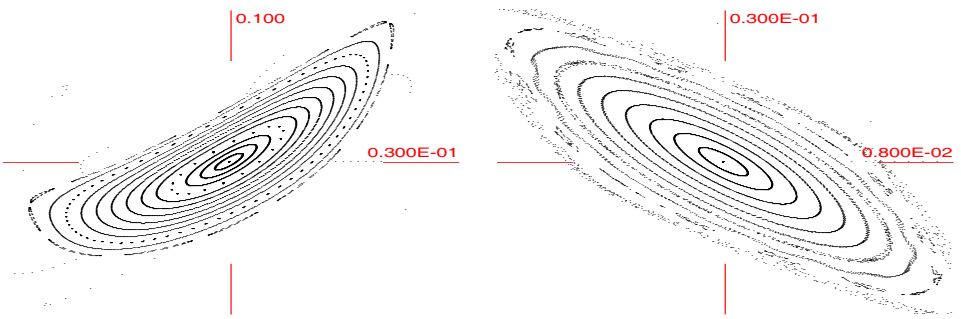

Fig. 10. Horizontal and vertical tracking in a model FFAG with fifth-order out of plane expansion, with EXPO symplectification. Left: $(x-a)$ plane, right: $(y-b)$ plane, where $a = p_x/p_0$, $b = p_y/p_0$ are normalized horizontal and vertical momenta correspondingly.

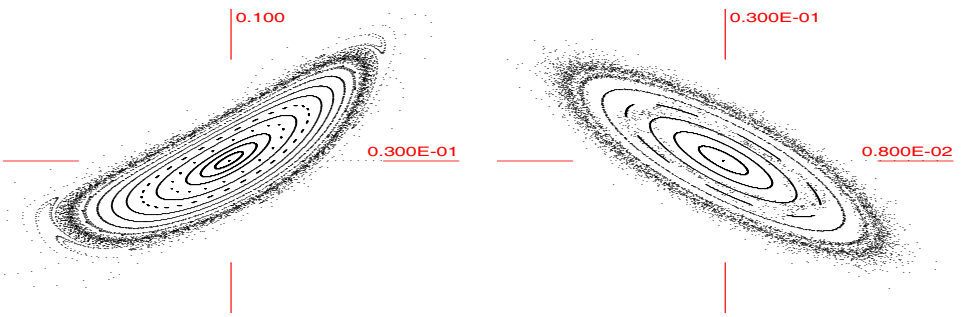

Fig. 11. Horizontal and vertical tracking in a model FFAG with eleventh-order out of plane expansion, without EXPO symplectification. Shows significant additional effects and different dynamic aperture compared to the lower order cases as seen in Figs. 2 to 5, suggesting that the low order methods for out-of-plane expansion and dynamics are not sufficient to capture the details of the dynamics. Left: $(x-a)$ plane, right: $(y-b)$ plane, where $a = p_x/p_0$, $b = p_y/p_0$ are normalized horizontal and vertical momenta correspondingly.

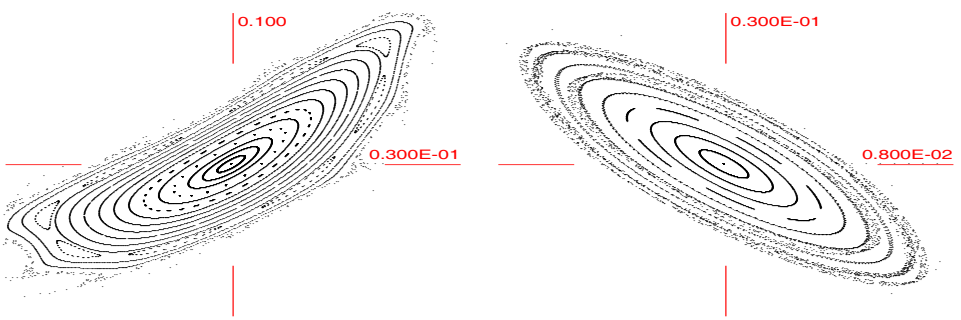

Fig. 12. Horizontal and vertical tracking in a model FFAG with eleventh-order out of plane expansion, with EXPO symplectification. Shows significant additional effects and different dynamic aperture compared to the lower order cases as seen in Figs. 2 to 5, suggesting that the low order methods for out-of-plane expansion and dynamics are not sufficient to capture the details of the dynamics. Left: $(x-a)$ plane, right: $(y-b)$ plane, where $a = p_x/p_0$, $b = p_y/p_0$ are normalized horizontal and vertical momenta correspondingly.

References

1. Chris Prior (Ed.). ICFA beam dynamics newsletter. Technical report, 2007.
2. M. K. Craddock. New concepts in FFAG design for secondary beam facilities and other applications. In *Proceedings, PAC05*, page 261, 2005.
3. Y. Mori. *Proceedings, FFAG05 Workshop*. FNAL, 2005.
4. K.R. Symon, D.W. Kerst, L.W. Jones, L.J. Laslett, and K.M. Terwilliger. Fixed-field alternating-gradient particle accelerators. *Physical Review*, 103:1837–1859, 1956.
5. Carol Johnstone and S. Koscielniak. *DPB Newsletter*, chapter The New Generation of FFAG Accelerators, pages 12–14. American Physical Society, 2008.
6. K. Makino and M. Berz. Effects of kinematic correction on the dynamics in muon rings. *AIP CP*, 530:217–227, 2000.
7. M. Berz, B. Erdélyi, and K. Makino. Fringe field effects in small rings of large acceptance. *Physical Review ST-AB*, 3:124001, 2000.
8. R Baartman et al. CYCLOPS. Technical report.
9. F. Meot. The ray-tracing code ZGOUBI. *Nuclear Instruments and Methods A*, 427:353–356, 1999.
10. F. Lemuet and F. Meot. Developments in the ray-tracing code ZGOUBI for 6-d multiturn tracking in FFAG rings, 2005.
11. T. Yokoi. Private communication.
12. M. Berz. *Modern Map Methods in Particle Beam Physics*. Academic Press, San Diego, 1999. Also available at http://bt.pa.msu.edu/pub.
13. M. Berz. Differential algebraic description of beam dynamics to very high orders. *Particle Accelerators*, 24:109, 1989.
14. M. Berz and K. Makino. COSY INFINITY Version 9.0 beam physics manual. Technical Report MSUHEP-060804, Department of Physics and Astronomy, Michigan State University, East Lansing, MI 48824, 2006. See also http://cosyinfinity.org.
15. M. Berz and K. Makino. COSY INFINITY Version 9.0 programmer's manual. Technical Report MSUHEP-060803, Department of Physics and Astronomy, Michigan State University, East Lansing, MI 48824, 2006. See also http://cosyinfinity.org.
16. M. Tawarmalani and N. Sahinidis. *Convexification and Global Optimization and Continuous and Mixed-Integer Programming*. Kluwer, 2002.
17. C. Floudas. *Nonlinear and Mixed-Integer Optimization*. Oxford University Press, 1995.
18. K. Lange. *Optimization*. Springer, 2004.
19. M. Berz, K. Makino, and Y.-K. Kim. Long-term stability of the Tevatron by validated global optimization. *Nuclear Instruments and Methods*, 558:1–10, 2005.
20. A. Poklonskiy. *Evolutionary Optimization Methods for Beam Physics*. PhD thesis, Michigan State University, East Lansing, Michigan, USA, 2008.
21. D. W. Kerst, E. A. Day, H. J. Hausman, R. O. Haxby, L. J. Laslett, F. E. Mills, T. Ohkawa, F. L. Peterson, E. M. Rowe, A. M. Sessler, J. N. Snyder, and W. A. Wallenmeyer. Electron model of a spiral sector accelerator. *Review of Scientific Instruments*, 31,10:1076–1106, 1960.
22. E. A. Crosbie. Use of the MURA transformation to generate the fields and calculate the motion of protons in the designed Argonne mini-aspun FFAG spiral sector accelerator. *IEEE Transactions on Nuclear Science*, NS-32, 5:2675–2677, 1985.
23. K. Makino. *Rigorous Analysis of Nonlinear Motion in Particle Accelerators*. PhD thesis, Michigan State University, East Lansing, Michigan, USA, 1998. Also MSUCL-1093.
24. S. L. Manikonda and M. Berz. Multipole expansion solution of the Laplace equation using surface data. *Nuclear Instruments and Methods*, 558,1:175–183, 2006.

25. S. L. Manikonda and M. Berz. An accurate high-order method to solve the Helmholtz boundary value problem for the 3D Laplace equation. *International Journal of Pure and Applied Mathematics*, 23,3:365–378, 2005.
26. S. L. Manikonda, M. Berz, and K. Makino. High-order verified solution of the 3D Laplace equation. *Transactions on Computers*, 4-11:1604–1610, 2005.
27. S. Manikonda. *High Order Finite Element Methods to Compute Taylor Transfer Maps*. PhD thesis, Michigan State University, East Lansing, Michigan, USA, 2006.
28. M. Lindemann. Rigorous field analysis of superconducting magnets and the influence on nonlinear dynamics in particle accelerators. Master's thesis, Michigan State University, East Lansing, Michigan, USA, 1998.
29. S. Manikonda, J. Nolen, M. Berz, K. Makino, and G.Weizman. Design of a superconducting quadrupole with elliptical acceptance and tunable higher order multipoles. Technical Report MSUHEP-060412, Department of Physics and Astronomy, Michigan State University, East Lansing, MI 48824, 2006.
30. M. Berz, B. Erdélyi, W. Wan, and K. Ng. Differential algebraic determination of high-order off-energy closed orbits, chromaticities, and momentum compactions. *Nuclear Instruments and Methods*, A427:310–314, 1999.
31. B. Erdélyi and M. Berz. Local theory and applications of extended generating functions. *International Journal of Pure and Applied Mathematics*, 11,3:241–282, 2004.
32. B. Erdélyi and M. Berz. Optimal symplectic approximation of Hamiltonian flows. *Physical Review Letters*, 87,11:114302, 2001.
33. B. Erdélyi. *Symplectic Approximation of Hamiltonian Flows and Accurate Simulation of Fringe Field Effects*. PhD thesis, Michigan State University, East Lansing, Michigan, USA, 2001.